ORIGINAL ARTICLE

JBMR®

Hox11 Function Is Required for Region-Specific Fracture Repair

Danielle R Rux,[1] Jane Y Song,[2] Kyriel M Pineault,[1] Gurjit S Mandair,[3] Ilea T Swinehart,[4] Aleesa J Schlientz,[4] Kayla N Garthus,[4] Steve A Goldstein,[5] Ken M Kozloff,[5] and Deneen M Wellik[1,4]

[1]Department of Cell and Developmental Biology, University of Michigan, Ann Arbor, MI, USA
[2]Cellular and Molecular Biology Program, University of Michigan, Ann Arbor, MI, USA
[3]Department of Biologic and Materials Sciences, School of Dentistry, University of Michigan, Ann Arbor, MI, USA
[4]Department of Internal Medicine, Division of Molecular Medicine and Genetics, University of Michigan, Ann Arbor, MI, USA
[5]Department of Orthopedic Surgery, University of Michigan, Ann Arbor, MI, USA

ABSTRACT

The processes that govern fracture repair rely on many mechanisms that recapitulate embryonic skeletal development. *Hox* genes are transcription factors that perform critical patterning functions in regional domains along the axial and limb skeleton during development. Much less is known about roles for these genes in the adult skeleton. We recently reported that *Hox11* genes, which function in zeugopod development (radius/ulna and tibia/fibula), are also expressed in the adult zeugopod skeleton exclusively in PDGFRα+/CD51+/LepR+ mesenchymal stem/stromal cells (MSCs). In this study, we use a *Hoxa11eGFP* reporter allele and loss-of-function *Hox11* alleles, and we show that *Hox11* expression expands after zeugopod fracture injury, and that loss of *Hox11* function results in defects in endochondral ossification and in the bone remodeling phase of repair. In *Hox11* compound mutant fractures, early chondrocytes are specified but show defects in differentiation, leading to an overall deficit in the cartilage production. In the later stages of the repair process, the hard callus remains incompletely remodeled in mutants due, at least in part, to abnormal bone matrix organization. Overall, our data supports multiple roles for *Hox11* genes following fracture injury in the adult skeleton. © 2017 American Society for Bone and Mineral Research.

KEY WORDS: SKELETAL INJURY/FRACTURE HEALING; MESENCHYMAL STROMAL/STEM CELLS; MOLECULAR PATHWAYS–DEVELOPMENT; *HOX* GENES; ENDOCHONDRAL OSSIFICATION–CARTILAGE

Introduction

The mammalian skeleton boasts a remarkable capacity for regeneration following injury. It is one of only a few postnatal processes that are truly regenerative, reestablishing original structure and function without scar formation. Interestingly, many of the mechanisms that govern fracture callus formation and remodeling include those that are also required during embryonic skeletal development.[1–5] The expression of several genes required for long-bone formation in the embryo (endochondral ossification) are also expressed in the fracture callus, and the patterns of expression and overall histology show similarities to those observed in the growth plate.[3–5] A group of transcription factors that have received little attention in this process are the *Hox* genes.

Hox genes are homeodomain-containing transcription factors that are required for region-specific patterning of the skeleton during development. They are expressed and function in spatially distinct domains along the anterior-posterior (AP) body axis and proximal-distal limb axis.[6–8] The 39 mammalian *Hox* genes are subdivided into 13 paralogous groups (*Hox1* to *Hox13*) based on sequence similarity and position within the *Hox* cluster. Genetic studies show that members of each paralogous group display a remarkable degree of functional redundancy with one another; loss of function of entire paralogous groups results in severe, region-specific skeletal defects along the AP axis.[8–15] The posterior *Hox* genes (*Hox9* to *Hox13)* were also co-opted in limbed vertebrates to function in proximal to distal patterning of the limbs.[10,15–20] The *Hox11* paralogs instruct proper development of the zeugopod elements of the limb skeleton (radius/ulna and tibia/fibula).[15–17] Loss of *Hox11* function results in severe patterning defects of the zeugopod while the remainder of the limb develops normally. Previous studies have reported *Hox* expression during fracture healing[21–23]; however, *Hox* gene function in this process has not been directly tested.

Received in original form November 23, 2016; revised form April 26, 2017; accepted May 1, 2017. Accepted manuscript online May 4, 2017.
Address correspondence to: Deneen M Wellik, PhD, University of Michigan Medical Center, 109 Zina Pitcher, 2053 BSRB, Ann Arbor, MI 48109-2200, USA. E-mail: dwellik@umich.edu
Current address: Ilea T Swinehart, MedPace Incorporated, Cincinnati, OH 45227, USA.
Current address: Aleesa J Schlientz, Institute of Molecular Biology, University of Oregon, Eugene, OR 97403, USA.
Additional Supporting Information may be found in the online version of this article.
Journal of Bone and Mineral Research, Vol. 32, No. 8, August 2017, pp 1750–1760
DOI: 10.1002/jbmr.3166

The maintenance of *Hox11* expression in the perichondrium/periosteum surrounding the developing skeletal elements of the limbs into late stages of embryonic development[24] led us to question whether *Hox* genes continue to be expressed and function beyond early patterning events in the embryo. Recently, we reported that *Hox11* genes are expressed exclusively in mesenchymal stem/stromal cells (MSCs) in the bone marrow and periosteum at adult stages.[25] Using a *Hoxa11eGFP* insertion allele, we demonstrated that Hoxa11eGFP+ cells are exclusively expressed in PDGFRα+, CD51+, and Leptin Receptor+ (LepR+) cells, markers that have been previously characterized to enrich for mesenchymal progenitor activity in bone marrow non-endothelial stroma and to contribute to fracture healing.[26–28] Importantly, we reported that the adult expression and function of *Hox11* genes is spatially restricted to same region in which these genes are expressed and function in the embryo (the zeugopod for *Hox11* in the limb skeleton), and that other adult *Hox* gene expression profiles also follow this pattern in other regions of the skeleton.[25,29] Together, this work suggests that *Hox* genes are expressed and function with regional specificity in adult skeletal MSCs.

In this study, we explore the defects associated with the loss of *Hox11* function in fracture repair using loss-of-function mouse models. At early stages of repair, we find that *Hox11* function is required for chondrocyte differentiation during fracture healing. In addition, we report evidence for bone modeling defects in *Hox11* mutants; these mutant fractures display defects in the remodeling phase of repair are unable to remodel to regain normal morphology. Our work is the first to demonstrate adult function(s) for *Hox11* genes in skeletal repair and regeneration following fracture injury.

Materials and Methods

Mice

All mice were maintained in a C57BL/6 background. Male and female mice either double-heterozygous or single-heterozygous for the *Hoxa11* and *Hoxd11* null alleles were mated to generate compound mutant animals.[16] All animals in the study were maintained on a C57/Bl6 background and group-housed in standard condition, unless separation was required due to fighting. Animals heterozygous for the *Hoxa11eGFP* allele were generated by traditional breeding strategies as described.[30] To assess spatial variation in bone fracture repair based on local *Hox* expression levels, three distinct fracture-healing models were employed: ulnar, tibial, and femoral. All animals were anesthetized with isoflurane during each procedure and provided buprenorphine preoperatively and postoperatively. Carprofen was also given during the recovery period. Postoperative radiographs were taken immediately following fracture (Faxitron X-Ray; Faxitron, Tucson, AZ, USA) to ensure proper fracture location. All animals were fully weight bearing within 1 hour following surgery. Full fracture methods are described in detail in the Supporting Information. All animal experiments described in this article were reviewed and approved by the University of Michigan's Committee on Use and Care of Animals, Protocol #PRO00006651 (Wellik) and Protocol #PRO00006763 (Goldstein).

Additional materials and methods may be found in the Supporting Information and include the following: fracture methods; X-ray and micro–computed tomography (μCT); histology; immunohistochemistry; and histomorphometric measurements and Raman spectroscopy.

Results

Hox11 is expressed throughout fracture repair

Fracture healing can be loosely defined by distinct phases of anabolic (callus expansion) and catabolic (callus remodeling) responses to the injury.[31,32] Resident MSCs in the skeleton (from the periosteum and bone marrow) provide the major source of progenitors for the repair process.[28,33–37] Hoxa11eGFP, at adult stages, is visualized in both the periosteum and bone marrow as a progenitor-enriched, non-endothelial, MSC population.[25] To explore a possible role for *Hox11* genes in the repair process, the expression of Hoxa11eGFP was examined following fracture injury of both the ulna or the tibia (forelimb or hindlimb zeugopod) using an anti-GFP antibody developed with alkaline phosphatase. Sections were developed without primary antibody to confirm that staining is specific (Supporting Fig. 1D). During hematoma formation (0.5 weeks postfracture [WPF]), Hoxa11eGFP+ cells begin to expand from the periosteum (Fig. 1*A*, Supporting Fig. 1A). During the soft (cartilage) callus (1.5 WPF) and hard (bony) callus (3 WPF) stages, significant expansion of Hoxa11eGFP+ cells throughout the callus is observed. Hoxa11eGFP+ cells are present at the center of the soft callus, in the medullary space at the site of injury, and in the expanded periosteal stromal layer that surrounds the newly formed fracture callus (Fig. 1*B*; Supporting Fig. 1B). At hard callus stages, Hoxa11eGFP+ cells are observed lining the woven bone surfaces (Fig. 1*C*). *Hox11* continues to be expressed well into remodeling stages as evidenced by extensive Hoxa11eGFP expression at 6 WPF (Supporting Fig. 1C). Importantly, our previous work shows that *Hox11*-expressing cells do not overlap with any markers of differentiated cells throughout the fracture healing process (including osteoblasts, osteoclasts, macrophages, endothelial cells, neurons, and chondrocytes), and flow cytometry demonstrates a cell-surface marker profile that is consistent with expression of Hoxa11eGFP exclusively in MSCs.[25]

Hox11 loss-of-function mice display defects during fracture healing

To assess a role for *Hox11* genes in the response to fracture injury, an ulnar fracture model was employed in *Hox11* compound mutants (referred to as *Hox11* mutant) in which three *Hox11* alleles are mutated. Retention of one wild-type allele is sufficient to prevent the developmental skeletal defects observed in four-allele mutant animals.[17,24] X-rays and μCT scans performed at several time points following fracture injury (in accordance with accepted protocols[38]) reveal abnormal fracture healing in *Hox11* mutants. During the early response to injury, 1.5 WPF, there are no apparent differences in ossification between mutants and controls (Fig. 2*A*). However, by mid-stage healing (3 WPF) *Hox11* mutant animals demonstrate a delay in fracture gap union (Fig. 2*B*).

During remodeling stages of healing (>6 WPF), two phenotypes are observed in *Hox11* mutant animals. First, a significant number of animals exhibit non-union fractures (Fig. 2*F*). Second, mutant animals that display fracture union demonstrate a dramatic delay in remodeling. Histological analyses reveal a significant amount of woven bone remaining in the bone marrow space at 6 and at 12 WPF compared to wild-type control fracture injuries that have remodeled this space by these time points (Fig. 2*C*, *D*). Notably, this incomplete remodeling remains at 21 WPF (Fig. 2*E*). μCT analyses support these observations. Although the callus volume of control fractures declines with

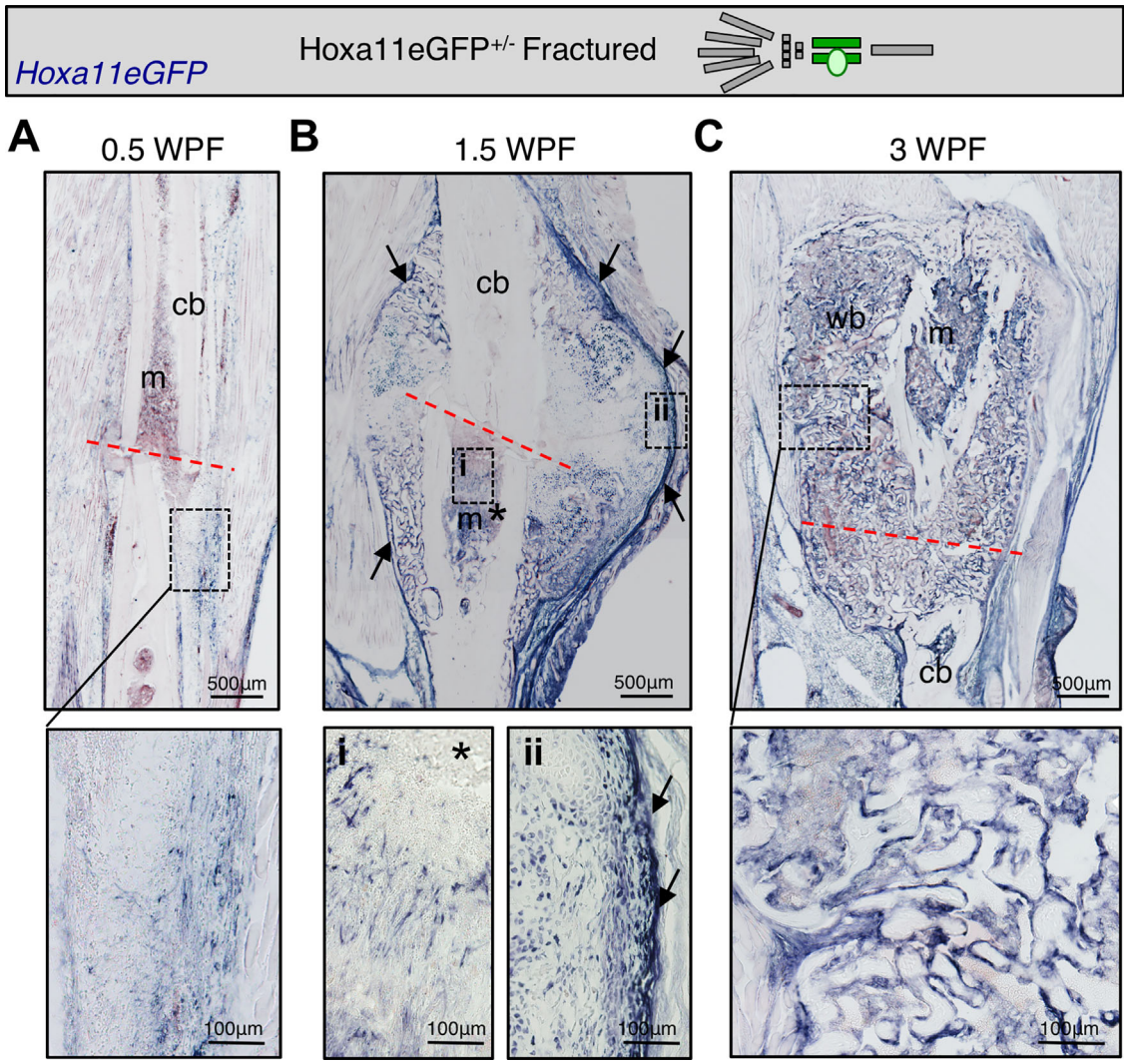

Fig. 1. *Hox11* is expressed throughout fracture injury in the limb zeugopod. Limb schematic depicts *Hoxa11eGFP* regional expression (green) and the fracture callus in the zeugopod region (tibia). *Hox11* expression is shown using a GFP primary antibody and developing with alkaline phosphatase. (*A*) *Hox11* is expressed at low levels in the hematoma. (*B*) *Hox11* expression expands at 1.5 WPF including the intramedullary space (*) and in the expanded periosteum surround the callus (arrows). (*C*) *Hox11* is expressed near woven bone surfaces in the hard callus at 3 WPF. WPF = weeks postfracture, cb = cortical bone, m = marrow/intramedullary space, wb = woven bone, red dashed line = fracture line.

time after injury, indicative of remodeling, the callus volume in *Hox11* mutant fracture injuries remains elevated (Fig. 2*G*).

Loss of *Hox11* function reduces chondrocyte differentiation in the early callus

Processes required for early callus formation were evaluated in order to understand the cellular mechanism for delayed callus bridging in *Hox11* mutant fracture injuries. New bone formation in the callus is accomplished by intramembranous and endochondral ossification, distinct processes that act simultaneously following fracture to promote repair at the site of injury.[1,31] Vascularization is critical for this process, and ischemic injuries result in non-union fractures that require medical intervention.[39,40]

In both control and mutant fracture injuries, new bone forms at the outer callus, along the periosteal surface, characteristic of intramembranous ossification (Fig. 3*A*, *B*). In both groups, these regions exhibit high levels of Osterix expression (a marker of osteoblasts) and are highly vascularized (platelet endothelial cell adhesion molecule [PECAM]) (Fig. 3*B*). No defects are observed in the overall vascularization of *Hox11* mutant calluses (Fig. 3*C*, *D*).

To evaluate endochondral ossification, histomorphometry measurements were performed on SafraninO/Fast Green-stained sections of early calluses. At three time points postfracture (1.5 WPF, 3 WPF, and 6 WPF), the proportion of the callus comprised of mesenchyme, cartilage, or woven bone was measured (Fig. 4*A*, *B*). Results reveal a decrease in woven bone and an increase in mesenchyme at the earliest stages of *Hox11* mutant callus formation compared to controls (Fig. 4*A*, *B*); a result consistent with delayed union observed by X-ray and µCT analyses (Fig. 2). Notably, a significant reduction in cartilage formation (Safranin O) is observed in *Hox11* mutant fractures at all stages examined (Fig. 4*A*, *B*).

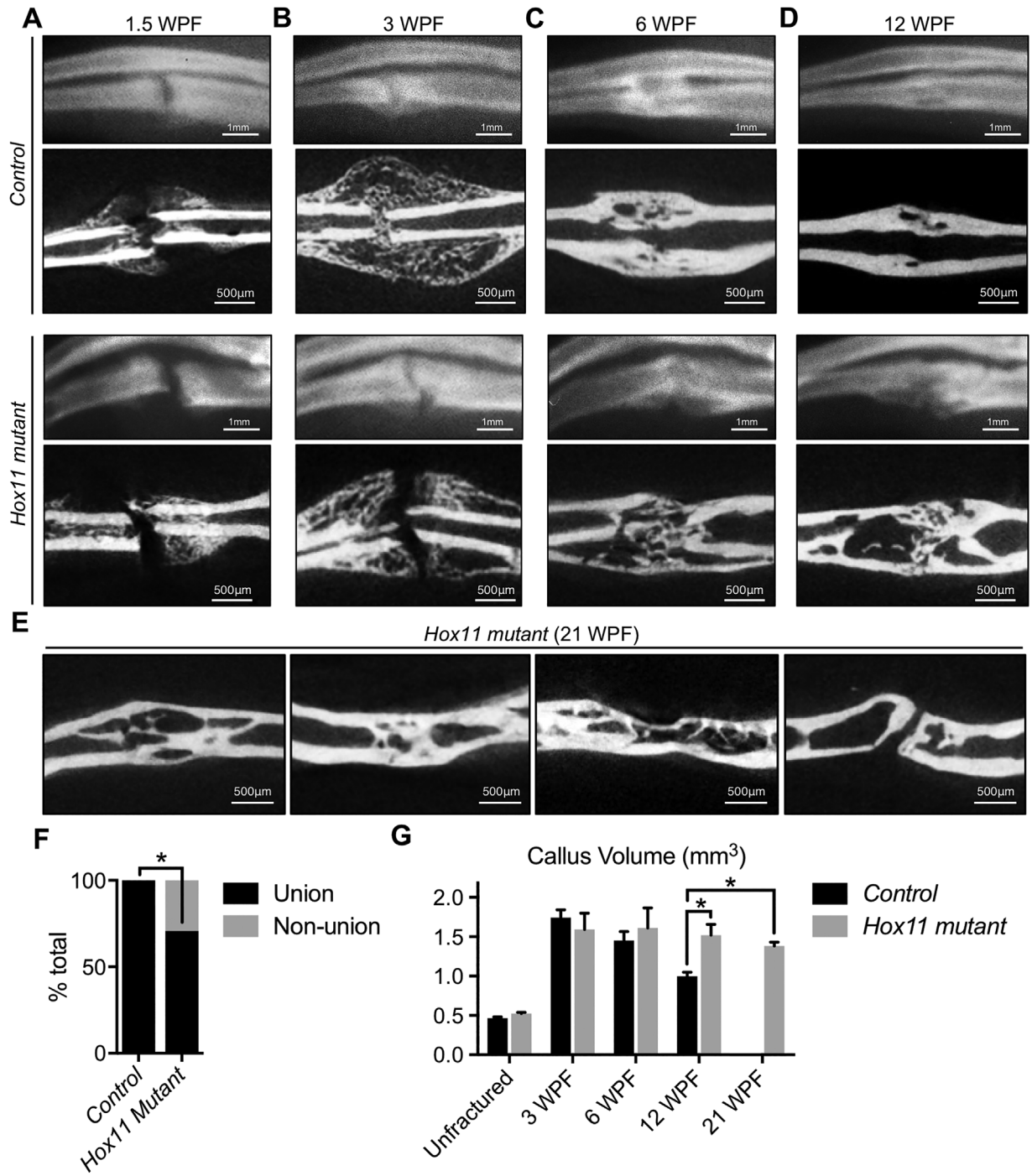

Fig. 2. Loss of *Hox11* function results in defects following fracture injury. (*A–D*) X-rays (top panels) and cross-sectional views of μCT (lower panels) in control and in *Hox11* mutant animals. (*A*) At 1.5 WPF, X-ray and μCT images are comparable between groups. (*B*) At 3 WPF, controls are bridged and mutants are not. (*C*, *D*) At 6 WPF and 12 WPF, most mutants are now bridged, but exhibit delayed remodeling compared to controls. (*E*) Cross-sectional views of μCT at 21 WPF persistent and incomplete bone remodeling in mutant animals. (*F*) 100% of control animals demonstrate union fractures compared to 71% of *Hox11* mutant animals. Statistical analysis carried out by two-tailed Fisher's exact test and by two-tailed chi-square test; $^{*}p < 0.05$. (*G*) μCT analysis shows statistically significant maintenance of callus volume at late stages in mutants. Statistical analysis carried out by Student's *t* test; $^{*}p < 0.05$. WPF = weeks postfracture.

To further understand the cartilage defect, immunohistochemistry was performed for specific markers of chondrogenic differentiation. Sox9 and Sox5, the earliest transcription factors expressed during chondrocyte differentiation, are expressed broadly in both control and *Hox11* mutant fracture calluses (Fig. 4*Ci*, Supporting Fig. 2A). However, mature cartilage markers, Collagen2a1 (resting, proliferating, and prehypertrophic chondrocytes) and Collagen10a1 (hypertrophic

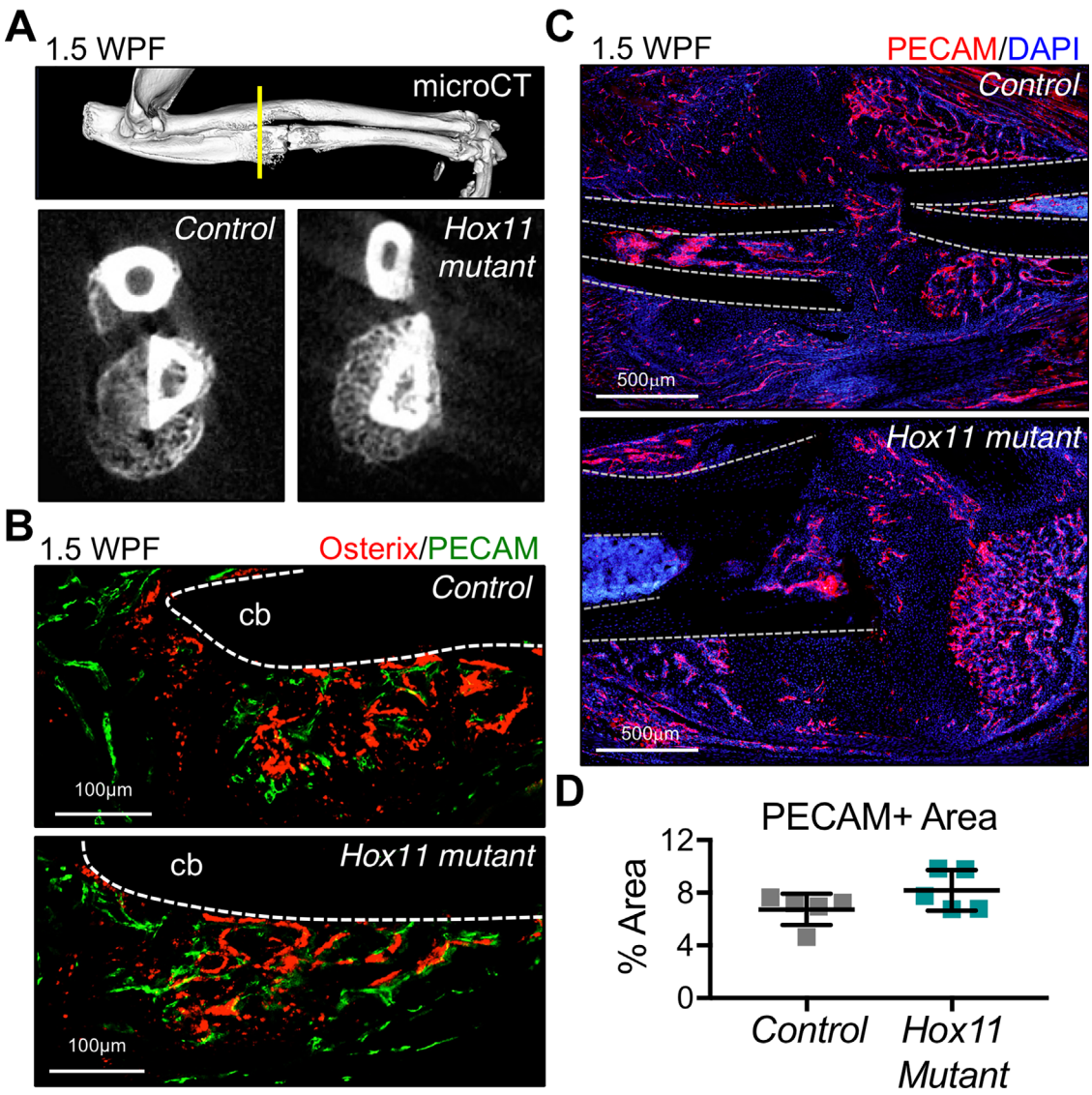

Fig. 3. Intramembranous ossification and vascularization are unchanged in *Hox11* mutant fractures. (*A*) μCT analysis of outer regions of callus show comparable bone formation in regions of intramembranous ossification. Yellow line shows approximate region of cross-sectional images. (*B*) Osterix and PECAM-stained sections show bone formation and vascularization in regions of intramembranous ossification. (*C*, *D*) PECAM-staining in controls and *Hox11* mutants shows comparable vascularization in the early callus (1.5 WPF). cb = cortical bone.

chondrocytes), are clearly reduced in mutants (Fig. 4*Cii–iii*). The ossification of cartilage as visualized by Von Kossa staining is abundant in control calluses and this is also significantly reduced in the *Hox11* mutant callus (Fig. 4*D*). Areas of mesenchyme can also be visualized at the center of *Hox11* mutant calluses by this method (Fig. 4*D*). Combined with the callus histomorphometry (increased mesenchyme and decreased Safranin O), these data indicate a defect in chondrocyte differentiation that limits endochondral ossification.

Bone modeling is disrupted to due loss of *Hox11* function

By late stages of repair, the majority of *Hox11* mutant animals demonstrate successful fracture union (Fig. 2*F*). However, during the remodeling phases of repair, mutant animals display a notable impairment as late as 21 WPF with all mutant animals retaining significant woven bone throughout the central callus region, unlike control animals that have largely re-established prefracture morphology by 12 WPF (Fig. 2*E*, *G*). To explore a possible cause for this phenotype, osteoclasts were examined. Quantification of tartrate resistant acid phosphatase (TRAP) reveals that osteoclasts are present at a similar density in control and mutant fracture injuries (Fig. 5*A*, *B*). Cathepsin K, an enzyme that functions in bone-resorbing osteoclasts,[41] is similarly expressed in both groups (Fig. 5*C*). However, close examination reveals many osteoclasts in *Hox11* mutant fracture injuries are enlarged and detached from the bone surface, which may contribute to incomplete remodeling of *Hox11* mutant fracture injuries (Fig. 5*D*). Maintained osteoid at the bone surface can explain such an observation; however, Von Kossa and basic fuchsin staining does not reveal differences in osteoid deposition between controls and mutants (Supporting Fig. 3).

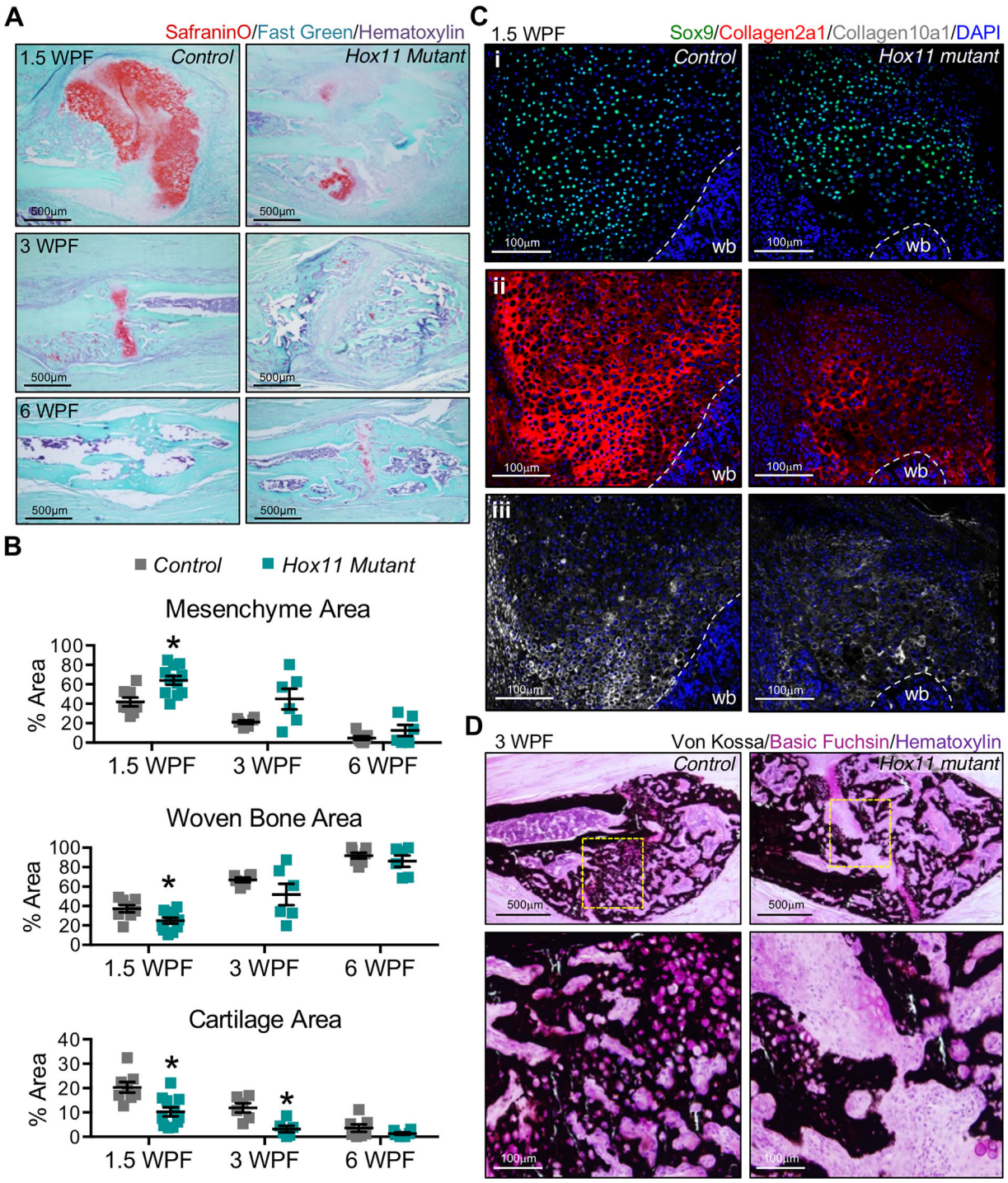

Fig. 4. Chondroctye differentiation and endochondral ossification is disrupted in the *Hox11* mutant callus. (*A*, *B*) Histomorphometric quantifications of the mesenchymal, woven bone and cartilage areas from Safranin O/Fast Green-stained sections at 1.5, 3, and 6 WPF. Cartilage was designated by Safranin O. Woven bone and mesenchyme were designated visually; the latter refers to non-woven bone, non-safranin O-positive area. Abundant cartilage formation is visualized in center regions of control calluses; mesenchyme is maintained in similar regions of mutant calluses. Statistical analysis carried out by Student's *t* test; $^{*}p < 0.05$. (*C*) Sox9, Collagen2a1 and Collagen 10a1-stained sections at 1.5 WPF show chondrocyte differentiation in control and mutant calluses. (*D*) Von Kossa–stained sections show unbridged callus at 3 WPF in mutant fractures and undifferentiated mesenchyme at the center of the callus. wb = woven bone; WPF = weeks postfracture.

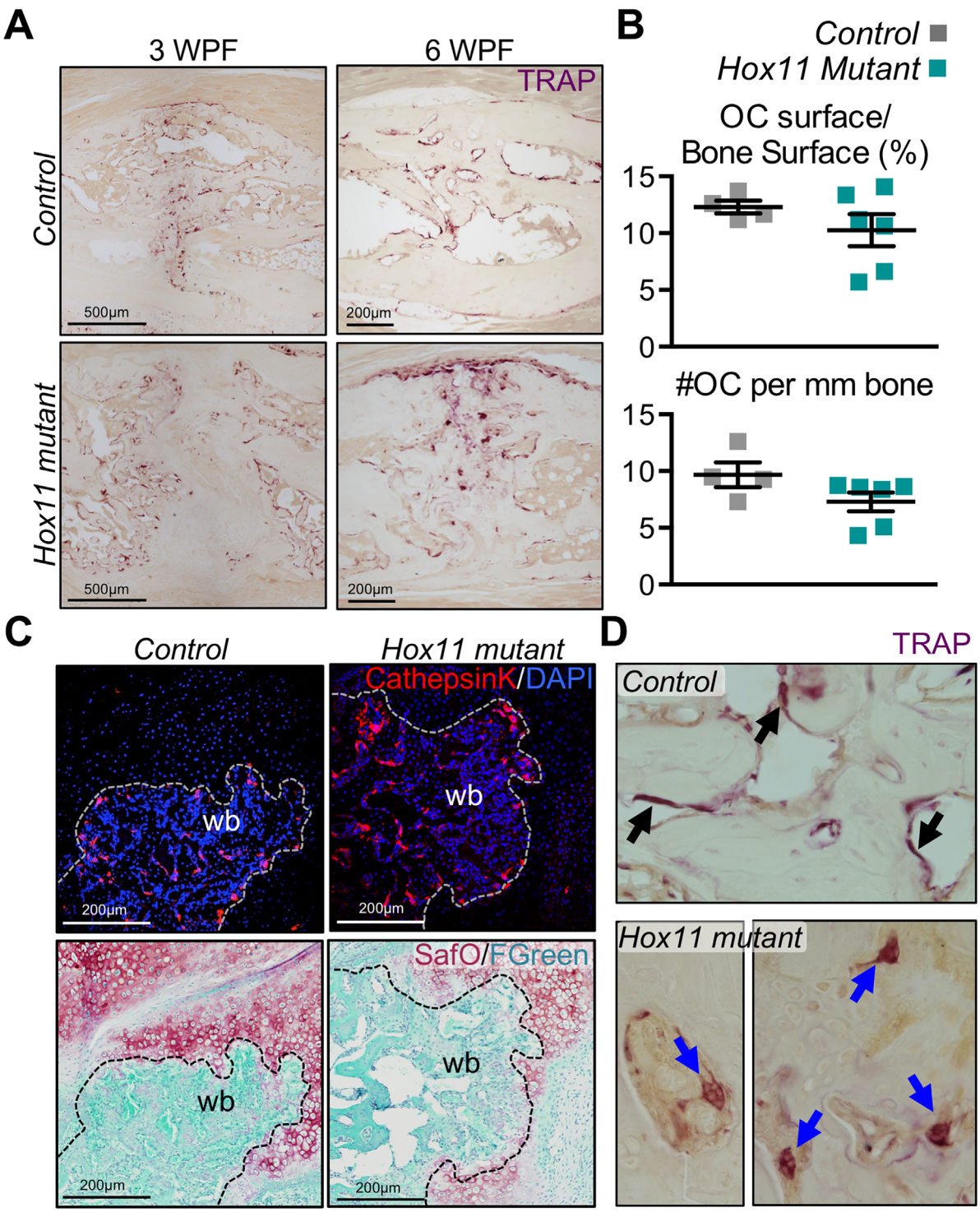

Fig. 5. Osteoclasts are present, express markers of resorption in the *Hox11* mutant callus. (*A*) TRAP-stained callus sections from control and *Hox11* mutant animals at 3 and 6 WPF show TRAP+ osteoclasts in calluses. (*B*) Histomorphometric quantification of osteoclasts per bone surface (%) and number of osteoclasts per 1mm of bone surface is comparable in controls and mutants. (*C*) Cathepsin K-stained callus sections from control and mutant animals show positive staining in controls and mutants. Safranin O/Fast Green staining on the same sections shows the overlap of CathepsinK with woven bone areas. (*D*) Images of large, detached osteoclasts in the *Hox11* mutant callus (blue arrows) compared to control osteoclasts that are flat and attached to the bone surface (black arrows). WPF = weeks postfracture, wb = woven bone.

Previous work demonstrates that *Hox11* genes are not expressed in hematopoietic cells at any stage of development or repair[24,25]; therefore, the defects associated with reduced osteoclast attachment are presumably non-cell autonomous, but may be caused by alterations in bony matrix. By μCT, measurements of bone and mineral density (BV/TV, BMD, BMC, and tissue mineral density [TMD]) are unchanged between controls and *Hox11* mutants at all time points examined (Table 1), and is consistent with a recent study of compound mutants through postnatal stages of development.[42] Raman spectroscopy was used to provide a more powerful analysis of possible bone matrix abnormalities in *Hox11* mutant animals. This unique and more sensitive tool is capable of assessing bone quality parameters by measuring relative changes in mineral-to-matrix ratios, mineral crystallinity, and collagen crosslink ratios, providing information on tissue-level material properties.[43] For this study, the technique was employed on woven bone in the fracture callus, and on cortical bone outside the callus in the fractured limb and on the contralateral limb. Analyses of these fractures show no statistically significant changes in mineral crystallinity, and are consistent with μCT results (Fig. 6*A*, Table 1).[42] However, mineral-to-matrix ratios in the cortical bone of *Hox11* mutants are significantly increased compared to controls (Fig. 6*B*). Together, these data are consistent with the absence of changes in mineralization, but abnormalities in the proper organization of bone matrix.

Specific matrix bands related to the collagen crosslinks ratio could not be analyzed by Raman spectroscopy in this study due to polymer interference of the poly(methyl methacrylate) (PMMA)-embedded specimens (data not shown). To further evaluate defects in matrix organization, Picrosirius Red staining combined with polarized light microscopy was performed.[44] Using this technique, an organized or directional matrix appears linear (green) under polarized light, whereas disorganized or multidirectional matrix (red/orange) yields a basket-weave appearance. New woven bone generated in the fracture callus is highly disorganized in both control and *Hox11* mutant calluses as is expected for this rapid bone deposition (Fig. 6*C*). However, *Hox11* mutant animals also display significant disorganization in their cortical bone matrix (Fig. 6*D*, Supporting Fig. 4). In controls, Sclerostin staining osteocytes are regularly spaced and well organized in the bone matrix (Fig. 6*E*). In *Hox11* mutants, however, osteocytes embedded in cortical bone exhibit irregular spacing and areas of aggregation within the bone matrix (Fig. 6*E*).

Discussion

Our understanding of *Hox* transcription factors in the skeleton is largely limited to embryonic development; however, recent studies have shown that *Hox* genes are re-expressed during repair, consistent with possible functions during fracture repair.[21–23,45] Transcriptome analyses have shown broad increases in the expression of various *Hox* genes throughout fracture repair of the femur.[21,22] Additionally, differential expression (and function) of *Hox* genes has been suggested as a cause for scar formation in a transplant study where periosteal progenitor cells from different anatomical locations were swapped in fracture injuries.[23] When Hox+ cells were transplanted into a mandibular injury (a site normally negative for *Hox*-expressing cells), chondrocytes formed and differentiated to cartilage at this injury site. This is a skeletal region that would have normally healed by intramembranous ossification. This supports a possible function for *Hox* genes in adult skeletal

Table 1. μCT Parameters Measured During Fracture Injury Repair

	Unfractured		1.5 weeks postfracture		3 weeks postfracture	
Measured parameter	*Control* ($n = 6$)	*Hox11 mutant* ($n = 8$)	*Control* ($n = 5$)	*Hox11 mutant* ($n = 8$)	*Control* ($n = 5$)	*Hox11 mutant* ($n = 6$)
Callus volume (mm^3)	0.45 (0.03)	0.52 (0.04)*	1.81 (0.45)	2.75 (0.72)*	1.74 (0.22)	1.59 (0.50)
Bone volume (mm^3)	0.32 (0.01)	0.35 (0.03)*	0.52 (0.13)	0.78 (0.22)*	0.57 (0.08)	0.57 (0.21)
BV/TV (%)	.71 (0.02)	0.67 (0.02)	.32 (0.18)	0.28 (0.03)	0.33 (0.05)	0.35 (0.05)
BMD (mg/cm^3)	839.6 (40.7)	740.2 (61.8)	486.0 (173.2)	424.1 (101.1)	511.3 (30.4)	480.2 (77.5)
BMC (mg)	.36 (0.01)	0.39 (0.05)	0.82 (0.15)	1.07 (0.31)	0.89 (0.08)	0.78 (0.32)
TMD (mg/cm^3)	977.0 (32.0)	905.6 (85.4)	935.3 (101.8)	860.7 (101.4)	838.0 (31.3)	792.5 (74.3)
	6 weeks postfracture		12 weeks postfracture		21 weeks postfracture	
Measured parameter	*Control* ($n = 5$)	*Hox11 mutant* ($n = 6$)	*Control* ($n = 5$)	*Hox11 mutant* ($n = 4$)	*Control* (ND)	*Hox11 mutant* ($n = 5$)
Callus volume (mm^3)	1.45 (0.25)	1.61 (0.62)	0.99 (0.12)	1.52 (0.27)*	ND	1.49 (0.16)*
Bone volume (mm^3)	0.79 (0.13)	0.81 (0.28)	0.63 (0.10)	0.93 (0.04)*	ND	0.86 (0.06)*
BV/TV (%)	0.55 (0.07)	0.51 (0.05)	0.64 (0.04)	0.63 (0.09)	ND	0.58 (0.04)
BMD (mg/cm^3)	664.3 (83.7)	606.4 (60.2)	796.2 (49.3)	817.7 (104.3)	ND	751.2 (24.3)
BMC (mg)	0.96 (0.17)	0.97 (0.34)	0.79 (0.13)	1.22 (0.07)*	ND	1.09 (0.12)*
TMD (mg/cm^3)	896.8 (48.6)	866.9 (37.1)	1036.2 (26.4)	1054.0 (72.6)	ND	983.3 (57.1)

Statistical analyses were carried out by Student's *t* test; *$p < 0.05$. Parameters measured include callus volume, total bone volume, BV/TV, BMD, BMC, and TMD.BV/TV = bone volume fraction; BMD = bone mineral density; BMC = bone mineral content; TMD = tissue mineral density; ND = no data collected.

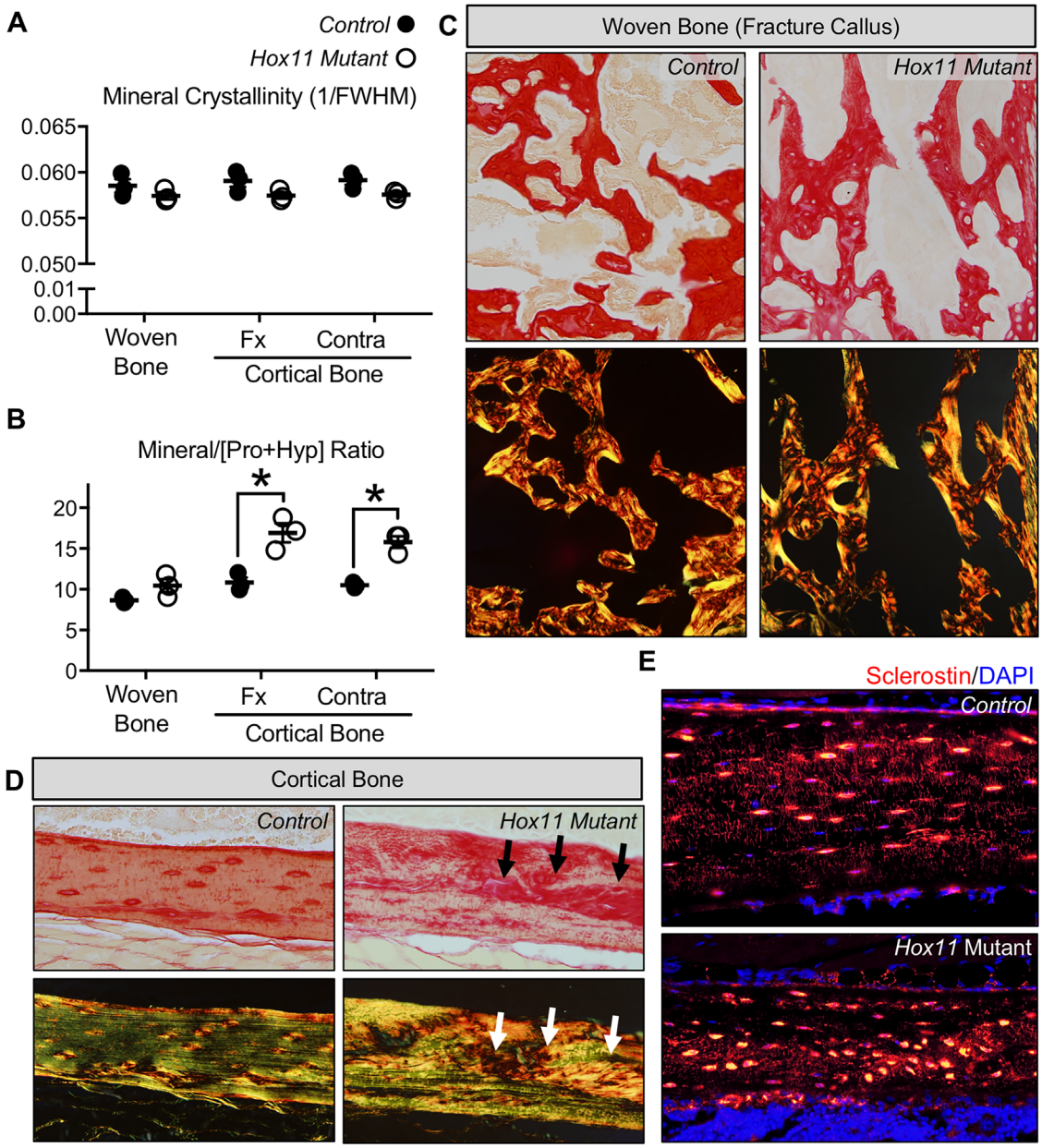

Fig. 6. Bone matrix organization is disrupted due to the loss of *Hox11* function. (*A*, *B*) Raman spectroscopy of woven bone callus and cortical bone outside the callus from controls and *Hox11* mutants at 3 WPF. Parameters measured include mineral crystalinity (*A*) and mineral to matrix [Pro+Hyp] ratio (*B*). Fx = fractured limb, Contra = contralateral limb. (*C*, *D*) Picrosirius red-stained sections with brightfield (top panels) or polarized light microscopy (bottom panels) for woven bone in fracture callus (*C*) and cortical bone out the callus (*D*). Arrows point to disorganized matrix in mutants. (*E*) Sclerostin-stained cortical bone shows disorganized osteocytes in *Hox11* mutants. WPF = weeks postfracture.

regeneration, but genetic loss-of-function analyses at endogenous sites of potential Hox activity have been lacking.

We report clear, regional expansion of *Hox11*-expressing cells in response to fracture injury of the zeugopod, the region of the skeleton that expresses *Hox11* genes during development. Complete loss of *Hox11* paralogous group function results in severe malformations during embryonic development and neonatal lethality that preclude adult studies. Using a sensitized background of compound *Hox11* loss-of-function animals, we show that loss of *Hox11* function results in defects in endochondral ossification during early callus formation and in impairment of the bone remodeling phase of repair.

We provide evidence that *Hox11* genes function in cartilage differentiation following fracture injury. The differentiation of *Hox*-expressing MSCs to chondrocytes during soft callus formation is disrupted. Mesenchyme is abundant in the *Hox11* mutant callus, and Sox9 and Sox5 (expressed in mesenchymal progenitors) are expressed broadly; however, downstream differentiation markers Collagen2a1, Collagen10a1, and Safranin O are markedly reduced. These combined data support that loss of *Hox11* function results in the failure of mesenchyme to differentiate to mature chondrocytes. Notably, these results are consistent with defects reported during embryonic limb formation with loss of *Hox11* function and with our more recent

work that demonstrates loss of chondrogenic differentiation in vitro from MSCs that carry these same mutations.[25,46] The decrease, but not complete absence, of cartilage in this fracture model is likely the result of incomplete loss of *Hox11* gene function (one wild-type remains in *Hox11* compound mutants).

We also show that loss of *Hox11* leads to defects during the remodeling phase after fracture injury. Osteoclasts are present, but many are detached from the bony matrix. Our observation of detached osteoclasts could be a result of changes in bone matrix disorganization in *Hox11* compound mutant animals, but this will require further study.

The restriction of paralogous group expression and function in skeletal patterning at specific anatomical locations during embryonic development is a key feature of *Hox* genes. The work described here supports a continued function for *Hox* genes in the vertebrate skeleton during adult fracture repair. Our previous worked showed that *Hox11* expression remains regionally restricted throughout postnatal growth, is maintained in the adult skeleton and expands in fracture injuries only in the zeugopod. Regional expression in the adult animal mirrors the pattern of expression and function during embryonic skeletal development. Importantly, we also reported that femur (stylopod) fracture injuries performed on *Hox11* loss-of-function animals display no defects in the repair process.[25] We would predict that different *Hox* paralogs perform similar activities at different anatomical locations. For example, *Hox10* paralogous group genes are required for patterning of the femur (stylopod) during embryonic development[10,15] and, given our work on *Hox11* genes, would likely be required for repair of these structures, but this has yet to be tested. Perhaps the most interesting question is whether different paralogs contribute in unique ways to the bone healing and remodeling process. Certainly, different *Hox* paralogs contribute to differential patterning information during embryonic development. This will be an important area for future study. Overall, our results suggest that regionally specific *Hox* function is an important and previously unappreciated mechanism required for successful fracture healing.

Disclosures

All authors state that they have no conflicts of interest.

Acknowledgments

This work was supported by NIH grants R01 AR061402 (DMW), T32 DE007057 (DRR, JYS, KMP), and T32 HD007505 (DRR, KMP), P30 AR069620 (Karl Jepsen, PI; David H. Kohn, Core Director), the 2016 Endowment for the Development of Graduate Education (EDGE, EBS-Michigan, DRR), the Bradley M Patten Fellowship (CDB-Michigan, DRR, KMP), and the University of Michigan Summer Biomedical and Life Sciences Fellowship (AJS). We thank Kathy Sweet, Bonnie Nolan, Charles Roehm, John Baker, Carol Whitinger, Basma Khoury, and Joseph Perosky of the Michigan Orthopedic Research Labs for technical support during fracture surgeries, plastic embedding and μCT analyses. We thank Yuji Mishina for guidance on Picrosirius Red staining. We also thank Drs. Benjamin Allen, Renny Franceschi, Karl Jepsen, Ernestina Schipani, Laurie McCauley, Daniel Lucas, and Michael Morris and numerous Wellik lab members for their advice and critique of the work.

Authors' roles: Study concept and design: DRR and DMW. Provision of study materials: DMW. Fracture model design: SAG and KMK. Data collection and experimentation: DRR, JYS, KMP, GSM, ILT, AJS, KNG. ILT, and AJS conducted many of the preliminary studies leading to this work. Data interpretation: DRR, ILT, GSM, SAG, KMK, and DMW. Manuscript writing: DRR and DMW. Revised manuscript content: AJS, GSM, SAG, KMK, and DMW.

References

1. Bolander ME. Regulation of fracture repair by growth factors. Proc Soc Exp Biol Med. 1992;200(2):165–70.
2. Einhorn TA. The cell and molecular biology of fracture healing. Clin Orthop Relat Res. 1998;355 Suppl:S7–21.
3. Ferguson C, Alpern E, Miclau T, Helms JA. Does adult fracture repair recapitulate embryonic skeletal formation? Mech Dev. 1999; 87(1-2): 57–66.
4. Gerstenfeld LC, Cullinane DM, Barnes GL, Graves DT, Einhorn TA. Fracture healing as a post-natal developmental process: molecular, spatial, and temporal aspects of its regulation. J Cell Biochem. 2003;88(5):873–84.
5. Vortkamp A, Pathi S, Peretti GM, Caruso EM, Zaleske DJ, Tabin CJ. Recapitulation of signals regulating embryonic bone formation during postnatal growth and in fracture repair. Mech Dev. 1998;71(1–2):65–76.
6. Duboule D. Temporal colinearity and the phylotypic progression: a basis for the stability of a vertebrate Bauplan and the evolution of morphologies through heterochrony. Dev Suppl. 1994;135–42.
7. Iimura T, Pourquie O. Collinear activation of Hoxb genes during gastrulation is linked to mesoderm cell ingression. Nature. 2006;442(7102):568–71.
8. Mallo M, Wellik DM, Deschamps J. Hox genes and regional patterning of the vertebrate body plan. Dev Biol. 2010;344(1):7–15.
9. Condie BG, Capecchi MR. Mice with targeted disruptions in the paralogous genes hoxa-3 and hoxd-3 reveal synergistic interactions. Nature. 1994;370(6487):304–7.
10. Fromental-Ramain C, Warot X, Lakkaraju S, et al. Specific and redundant functions of the paralogous Hoxa-9 and Hoxd-9 genes in forelimb and axial skeleton patterning. Development. 1996;122(2): 461–72.
11. Horan GS, Ramirez-Solis R, Featherstone MS, Wolgemuth DJ, Bradley A, Behringer RR. Compound mutants for the paralogous hoxa-4, hoxb-4, and hoxd-4 genes show more complete homeotic transformations and a dose-dependent increase in the number of vertebrae transformed. Genes Dev. 1995;9(13):1667–77.
12. Kostic D, Capecchi MR. Targeted disruptions of the murine Hoxa-4 and Hoxa-6 genes result in homeotic transformations of components of the vertebral column. Mech Dev. 1994;46(3):231–47.
13. van den Akker E, Fromental-Ramain C, de Graaff W, et al. Axial skeletal patterning in mice lacking all paralogous group 8 Hox genes. Development. 2001;128(10):1911–21.
14. Wellik DM. Hox genes and vertebrate axial pattern. Curr Top Dev Biol. 2009;88:257–78.
15. Wellik DM, Capecchi MR. Hox10 and Hox11 genes are required to globally pattern the mammalian skeleton. Science. 2003;301(5631): 363–7.
16. Boulet AM, Capecchi MR. Multiple roles of Hoxa11 and Hoxd11 in the formation of the mammalian forelimb zeugopod. Development. 2004;131(2):299–309.
17. Davis AP, Witte DP, Hsieh-Li HM, Potter SS, Capecchi MR. Absence of radius and ulna in mice lacking hoxa-11 and hoxd-11. Nature. 1995;375(6534):791–5.
18. Fromental-Ramain C, Warot X, Messadecq N, LeMeur M, Dolle P, Chambon P. Hoxa-13 and Hoxd-13 play a crucial role in the patterning of the limb autopod. Development. 1996;122(10): 2997–3011.

19. Izpisua-Belmonte JC, Duboule D. Homeobox genes and pattern formation in the vertebrate limb. Dev Biol. 1992;152(1):26–36.
20. Zakany J, Duboule D. The role of Hox genes during vertebrate limb development. Curr Opin Genet Dev. 2007;17(4):359–66.
21. Bais M, McLean J, Sebastiani P, et al. Transcriptional analysis of fracture healing and the induction of embryonic stem cell-related genes. PLoS One. 2009;4(5):e5393.
22. Gersch RP, Lombardo F, McGovern SC, Hadjiargyrou M. Reactivation of Hox gene expression during bone regeneration. J Orthop Res. 2005;23(4):882–90.
23. Leucht P, Kim JB, Amasha R, James AW, Girod S, Helms JA. Embryonic origin and Hox status determine progenitor cell fate during adult bone regeneration. Development. 2008;135(17):2845–54.
24. Swinehart IT, Schlientz AJ, Quintanilla CA, Mortlock DP, Wellik DM. Hox11 genes are required for regional patterning and integration of muscle, tendon and bone. Development. 2013;140(22):4574–82.
25. Rux DR, Song JY, Swinehart IT, et al. Regionally restricted Hox function in adult bone marrow multipotent mesenchymal stem/stromal cells. Dev Cell. 2016;39(6):653–66.
26. Kunisaki Y, Bruns I, Scheiermann C, et al. Arteriolar niches maintain haematopoietic stem cell quiescence. Nature. 2013;502(7473):637–43.
27. Pinho S, Lacombe J, Hanoun M, et al. PDGFRalpha and CD51 mark human nestin+ sphere-forming mesenchymal stem cells capable of hematopoietic progenitor cell expansion. J Exp Med. 2013;210(7):1351–67.
28. Zhou BO, Yue R, Murphy MM, Peyer JG, Morrison SJ. Leptin-receptor-expressing mesenchymal stromal cells represent the main source of bone formed by adult bone marrow. Cell Stem Cell. 2014;15(2):154–68.
29. Rux DR, Wellik DM. Hox genes in the adult skeleton: novel functions beyond embryonic development. Dev Dyn. 2017;246(4):310–7.
30. Nelson LT, Rakshit S, Sun H, Wellik DM. Generation and expression of a Hoxa11eGFP targeted allele in mice. Dev Dyn. 2008;237(11):3410–6.
31. Schindeler A, McDonald MM, Bokko P, Little DG. Bone remodeling during fracture repair: the cellular picture. Semin Cell Dev Biol. 2008;19(5):459–66.
32. Einhorn TA, Gerstenfeld LC. Fracture healing: mechanisms and interventions. Nat Rev Rheumatol. 2015;11(1):45–54.
33. Colnot C. Skeletal cell fate decisions within periosteum and bone marrow during bone regeneration. J Bone Miner Res. 2009;24(2):274–82.
34. Mizoguchi T, Pinho S, Ahmed J, et al. Osterix marks distinct waves of primitive and definitive stromal progenitors during bone marrow development. Dev Cell. 2014;29(3):340–9.
35. Nakahara H, Bruder SP, Goldberg VM, Caplan AI. In vivo osteochondrogenic potential of cultured cells derived from the periosteum. Clin Orthop Relat Res. 1990;(259):223–32.
36. Park D, Spencer JA, Koh BI, et al. Endogenous bone marrow MSCs are dynamic, fate-restricted participants in bone maintenance and regeneration. Cell Stem Cell. 2012;10(3):259–72.
37. Worthley DL, Churchill M, Compton JT, et al. Gremlin 1 identifies a skeletal stem cell with bone, cartilage, and reticular stromal potential. Cell. 2015;160(1–2):269–84.
38. Bouxsein ML, Boyd SK, Christiansen BA, Guldberg RE, Jepsen KJ, Muller R. Guidelines for assessment of bone microstructure in rodents using micro-computed tomography. J Bone Miner Res. 2010;25(7):1468–86.
39. Colnot C, Lu C, Hu D, Helms JA. Distinguishing the contributions of the perichondrium, cartilage, and vascular endothelium to skeletal development. Dev Biol. 2004;269(1):55–69.
40. Hausman MR, Schaffler MB, Majeska RJ. Prevention of fracture healing in rats by an inhibitor of angiogenesis. Bone. 2001;29(6):560–4.
41. Saftig P, Hunziker E, Wehmeyer O, et al. Impaired osteoclastic bone resorption leads to osteopetrosis in cathepsin-K-deficient mice. Proc Natl Acad Sci U S A. 1998;95(23):13453–8.
42. Pineault KM, Swinehart IT, Garthus KN, et al. Hox11 genes regulate postnatal longitudinal bone growth and growth plate proliferation. Biol Open. 2015;4(11):1538–48.
43. Mandair GS, Morris MD. Contributions of Raman spectroscopy to the understanding of bone strength. Bonekey Rep. 2015;4:620.
44. Junqueira LC, Bignolas G, Brentani RR. Picrosirius staining plus polarization microscopy, a specific method for collagen detection in tissue sections. Histochem J. 1979;11(4):447–55.
45. Wang KC, Helms JA, Chang HY. Regeneration, repair and remembering identity: the three Rs of Hox gene expression. Trends Cell Biol. 2009;19(6):268–75.
46. Gross S, Krause Y, Wuelling M, Vortkamp A. Hoxa11 and Hoxd11 regulate chondrocyte differentiation upstream of Runx2 and Shox2 in mice. PLoS One. 2012;7(8):e43553.